Aging-Associated Enzyme Human Clock-1: Substrate-Mediated Reduction of the Diiron Center for 5-Demethoxyubiquinone Hydroxylation[†]

Tsai-Te Lu, **Seung Jae Lee**, **Ulf-Peter Apfel**, and **Stephen J. Lippard**[*]
Department of Chemistry, Massachusetts Institute of Technology, Cambridge, MA 02139, United States

Abstract

The mitochondrial membrane-bound enzyme Clock-1 (CLK-1) extends the average longevity of mice and *C. elegans*, as demonstrated for Δ*clk-1* constructs for both organisms. Such an apparent impact on aging and the presence of a carboxylate-bridged diiron center in the enzyme inspired the present work. We expressed a soluble human CLK-1 (hCLK-1) fusion protein with an N-terminal immunoglobulin binding domain of protein G (GB1). Inclusion of the solubility tag allowed for thorough characterization of the carboxylate-bridged diiron active site of the resulting GB1-hCLK-1 by spectroscopic and kinetic methods. Both UV-vis and Mössbauer experiments provide unambiguous evidence that GB1-hCLK-1 functions as a 5-demethoxyubiquinone-hydroxylase (DMQ-hydroxylase), utilizing its carboxylate-bridged diiron center. The binding of DMQ_n (n = 0 or 2) to GB1-hCLK-1 mediates reduction of the diiron center by NADH and initiates O_2 activation for subsequent DMQ hydroxylation. Deployment of DMQ to mediate reduction of the diiron center in GB1-hCLK-1 improves substrate specificity and diminishes consumption of NADH that is uncoupled from substrate oxidation. Both V_{max} and k_{cat}/K_M for DMQ hydroxylation increase when DMQ_0 is replaced by DMQ_2 as substrate, which demonstrates that an isoprenoid side chain enhances enzymatic hydroxylation and improves catalytic efficiency.

Although the average human lifespan has increased steadily over the past two centuries, factors governing the aging process with its concomitant frailty and disease remain uncertain.[1] An attempt to establish a model for studying the aging process led to the discovery of Clock-1 (CLK-1), an aging-associated enzyme.[2] CLK-1 is conserved in yeast, *C. elegans*, and mammals including rats, mice, and humans.[3] An increased lifespan, up to 30%, occurs in Δ*clk-1 C. elegans* and mice.[2,4] Long-lived *clk-1*^{+/-} mice containing lower CLK-1 levels display decreased activity of the mitochondrial electron transport chain, reduced ATP synthesis, and increased mitochondrial oxidative stress.[4] Impaired mitochondrial electron transport is accompanied by accumulation of 5-demethoxyubiquinone (DMQ), an immediate precursor of ubiquinone (UQ), as exhibited in mouse embryonic stem cells containing a knockout of *clk-1*.[5] During respiration, UQ mediates delivery of electrons from Complex I or II to Complex III within the inner mitochondrial membrane of eukaryotes via interconversion of oxidized quinone and reduced hydroquinone.[6]

[*]To whom correspondence should be addressed lippard@mit.edu. Phone: (617) 253-1892. Fax: (617) 258-8150.

Supporting Information
Additional details of the characterization of GB1-hCLK-1. This material is available free of charge via the Internet at http://pubs.acs.org.

Based on the accumulation of 5-demethoxyubiquinone (DMQ_9) in $\Delta clk\text{-}1$ mutants of *C. elegans* and mice, where the subscript indicates the length of the isoprenoid side chain (Chart 1), CLK-1 was proposed to function as a DMQ hydroxylase involved in the penultimate step of UQ biosynthesis.[5,7] DMQ is converted to UQ by CLK-1 hydroxylation and subsequent *O*-methylation by Coq3, an *O*-methyltransferase.[8] A structural model of CLK-1 from *P. aeruginosa* using bacterioferritin as a template revealed a four-helix bundle and, in addition, suggested a diiron active site within a conserved $EX_{n1}EXXHX_{n2}EX_{n3}EXXH$ binding motif.[9-10] This motif is shared by the hydroxylase components in soluble methane monooxygenase (sMMO), toluene monooxygenase (ToMO), phenol hydroxylase (PH), and ribonucleotide reductase, supporting the hypothesis that CLK-1 is a member of the carboxylate-bridged diiron protein family (Supplementary Fig. S1).[11-12] In addition, the structural model of human CLK-1 (hCLK-1) contains two conserved tyrosine residues having $Fe\cdots O_{Tyr}$ distances of 4.0 Å (Supplementary Fig. S1), reminiscent of the single conserved tyrosine responsible for radical initiation in ribonucleotide reductase.[11,13] Thus far, the function of the tyrosine residues in CLK-1 remains unexamined. A docking model of rat CLK-1 with its substrate, DMQ_{10}, was also reported.[10] A previously proposed structural model of rat CLK-1 suggested several key structural features involving interactions between the substrate and the protein.[10] Hydrophobic interactions occurring between the isoprenoid side chain of DMQ_{10} and a hydrophobic pocket within rat CLK-1 were proposed. In addition, hydrogen bonding between the carbonyl/methoxy group of DMQ_{10} and the protein motif $Glu_{22}/His_{110}/Tyr_{111}$ were postulated for the DMQ_{10} adduct of CLK-1 (Supplementary Fig. S1).

In the present study we report a robust expression system for, and substantially improved characterization of, CLK-1 as a follow-up of our preliminary work on this system.[14] The solubility of the hCLK-1 membrane-bound enzyme was significantly improved through construction of an N-terminal immunoglobulin binding domain of protein G (GB1) fusion protein. The fusion protein designed and investigated here could be expressed in a highly efficient manner in *E. coli*.[15] GB1-hCLK-1 uses its carboxylate-bridged diiron center to catalyze the hydroxylation of DMQ_0 (Chart 1). Reduction of the diiron center by NADH occurs via a quinone-mediated electron transfer process, without the need for an additional reductase protein. As demonstrated here, DMQ mediates reduction of diiron center for subsequent O_2 activation and DMQ hydroxylation in hCLK-1.

Material and Methods

Distilled water was purified with a Milli-Q filtering system. 2-Methoxy-5-methyl-1,4-benzoquinone (DMQ_0), 2-methoxy-3-hydroxyl-5-methyl-1,4-benzoquinone (DMQ_0-OH) and DMQ_2 were synthesized based on published procedures.[16-17] Other reagents were purchased from Sigma Aldrich and used as received.

Cloning and Plasmid Construction

The pET30a(+)-GBFusion vector was purchased from Dana-Farber/Harvard Cancer Center DNA resource core in Harvard medical school. pOTB7 containing human *clk-1* (*hclk-1*) gene was obtained from ATCC and used as the starting vector (ATCC number: MGC-671). A PCR was run to amplify the human *hclk-1* gene and introduce BamHI and EcoRI restriction sites into the 5' and 3' ends of the product using primers 5'-*hclk-1* (5'-TCAGGAGGATCCATGACTTTAGACAATATCAGT-3') and 3'-*hclk-1* (5'-CACACTGAATTCTTATAATCTTTCTGATAAATA-3'). The gene product was digested with BamHI and EcoRI for 2.5 h at 37 °C and purified by extraction from a 1.5 % agarose gel (Qiagen). The digested product was then ligated into pET30a(+)-GBFusion vector that had also been treated with the same enzymes using 1 μL of T4 DNA ligase (New England Biolabs) and incubated at 16 °C for 16 hr. A 3 μL portion of the ligation reaction solution

was transformed into *E. coli* DH5α cells (Invitrogen). The constructed plasmids were examined by agarose gel electrophoresis and then sequenced by the MIT Biopolymers facility.

Expression and Purification of GB1-hCLK-1

E. coli ArcticExpress(DE3)RP cells transformed with pET30a(+)-GBFusion-hclk-1 were cultured in 6 L of LB medium containing 50 μg/mL kanamycin at 37 °C until OD_{600} reached 0.4. Protein expression was induced by addition of IPTG to a final concentration of 100 μM. To maximize iron incorporation in recombinant GB1-hCLK-1, 100 μM $(NH_4)_2Fe(SO_4)\cdot 6H_2O$ was added to the culture every hour in the first three hours. Growth was continued for 16 h at 25 °C. Cells were collected by centrifugation at 4 °C, and the cell paste was frozen in liquid nitrogen and stored at -80 °C. The cell paste (~25 g) was sonicated on ice using a Branson sonifier for 10 min (3 sec on, 20 sec off) at 48 % output in 200 mL of 20 mM Tris, 100 μM $(NH_4)_2Fe(SO_4)_2\cdot 6H_2O$, 8 mM sodium thioglycolate, 2 mM cysteine, and 10% glycerol (buffer A, pH 7.0) containing 5 μL DNase I, 5 mM $MgCl_2$ and 50 μM PMSF. Insoluble material was removed by centrifugation at 16,000 g for 90 min, and the supernatant was filtered through a 0.22 μm membrane and loaded onto a DEAE Sepharose FF column (500 mL, 5 cm diameter × 25 cm length) equilibrated in buffer A. The column was washed with 500 mL of buffer A and then eluted in 2500 mL by running a linear gradient from 20 mM NaCl to 500 mM NaCl at a rate of 3.0 mL/min. Fractions containing GB1-hCLK-1 eluted at ~ 250 mM NaCl were identified by SDS-PAGE. These fractions were pooled and concentrated to ~12 mL using a 3K MWCO Amicon filter (Millipore, Inc.). The resulting protein was loaded onto a Superdex S75 column (320 mL, 2.6 cm diameter × 60 cm length) equilibrated in 20 mM Tris, 10 % glycerol (buffer B, pH 7.0). Proteins were eluted by running buffer B over the column at a flow rate of 1 mL/min. These fractions were pooled and loaded onto a Mono Q column (20 mL, 1.6 cm diameter × 10 cm length) equilibrated with buffer B. The column was washed with 40 mL of buffer B and then eluted in 400 mL by running a linear gradient from 20 mM NaCl to 500 mM NaCl at a rate of 0.5 mL/min. Purified GB1-hCLK-1 confirmed by SDS-PAGE was concentrated and stored at -80 °C until further use.

Determination of Protein Concentration, Iron Content, and Oligomeric State of GB1-hCLK-1

The concentration of GB1-hCLK-1 was determined by a Bradford protein assay using BSA as the standard. Iron content was measured by inductively coupled plasma/optical emission spectroscopy with calibration using an Fe standard (BDH, ARISTAR® PLUS). GB1-hCLK-1 was digested by 1 mL of 2% HNO_3 (BDH, ARISTAR® PLUS) and the precipitated protein was removed by centrifugation (13,000 rpm, 10 min). The supernatant was further diluted with 2% HNO_3 and analyzed by ICP-OES at the MIT Center for Materials Science and Engineering. The oligomeric state of GB1-hCLK-1 was determined with the use of a HiLoad™ 16/60 Superdex™ 200 prep grade (GE Healthcare) size exclusion column. The elution time of GB1-hCLK-1 (74 min) falls between those of BSA (66 kDa, 60 min) and carbonic anhydrase (29 kDa, 80 min), suggesting that GB1-CLK-1 is dimeric in 20 mM Tris, 10% glycerol, pH 7.0 buffer. All concentrations of GB1-hCLK-1 in this work are computed on the basis of the monomer unit molecular weight.

Hydroxylase Activity GB1-hCLK-1

GB1-hCLK-1 hydroxylase activity was studied by product characterization using GC-MS. An aliquot (0.5 mL) of reaction solution containing 5 μM GB1-hCLK-1, 1 mM NADH, and 1 mM DMQ_0 was quenched with 150 μL 0.7 M TCA after 30 min. The precipitated protein was removed by centrifugation. A 200 μL volume of chloroform was used to extract organic compounds from the supernatant, and the organic layer was analyzed by GC using an

ZB-5MSi column (Phenomenex) attached to an Agilent 6890N gas chromatography system. The following temperature sequence was applied to analyze the products: 60 °C for 1 min, 15 °C per min to 100 °C, hold at 100 °C for 10 min, 20 °C per min to 260 °C. DMQ eluted at 17.10 min and the DMQ-OH at 17.39 min.

Steady State Activity of GB1-hCLK-1

The steady state activity of GB1-hCLK-1 was characterized by an NADH consumption assay using an HP 8452 diode array spectrophotometer. For DMQ_0 (or DMQ_2) concentration-dependence assays, 200 μM of NADH was added to 5 μM of GB1-hCLK-1 and DMQ_0 (or DMQ_2) at a specified concentration and the change in absorbance at 340 nm was monitored. All reactions were monitored continuously at 340 nm ($\varepsilon_{340} = 6,220$ $M^{-1}cm^{-1}$). Reaction mixtures were held at a constant temperature of 25.0 °C using a circulating water bath. Data were analyzed by fitting the initial time points to the linear function.

Redox Titration of GB1-hCLK-1

A redox titration was performed to determine the number of equivalents of electrons necessary to fully reduce GB1-hCLK-1. A 100-μM solution of GB1-hCLK-1 was made anaerobic with 12-15 cycles of vacuum gas exchange with O_2 free N_2. This solution was then titrated with 5 μL aliquots of 3.3 mM $Na_2S_2O_4$ or 5 μL aliquots of 5 mM NADH in the presence of 100 μM DMQ_0. The decrease in absorbance at 340 nm was monitored 10 min after addition of dithionite (or NADH) by UV/vis spectroscopy.

Redox Potential Determination for GB1-hCLK-1

The equilibrium midpoint potentials of GB1-hCLK-1 were determined by a series of reductive titrations based on a reported procedure using methylene blue as a redox indicator dye.[18-19] GB1-hCLK-1 (ca. 20 μM) and dye (ca. 20 μM methylene blue) in a total volume 0.5 mL (100 mM Tris, pH 7.0) were made anaerobic with 12-15 cycles of vacuum gas exchange using O_2-free N_2 and titrated by a solution of sodium dithionite (ca. 500 μM). Multiple scans were taken after each dithionite addition until the system had reached equilibrium (usually 5-10 min, but as long as 40 min). The final spectrum was saved for data analysis. This process was repeated until the protein and dye were fully reduced. The solution potential and GB1-hCLK-1 midpoint potentials were computed for each titration point using modified Nernst equations (eq 1).[18-19]

$$E = E_{dye}^{o'} - \frac{RT}{n_{dye}F} \ln\left(\frac{dye_{red}}{dye_{ox}}\right) = E_i^{o'} - \frac{RT}{n_iF} \ln\left(\frac{i_{red}}{i_{ox}}\right) \quad (1)$$

Kinetic Studies of Substrate-Mediated Reduction of Oxidized GB1-hCLK-1

Reduction of oxidized GB1-hCLK-1 was monitored by using a HiTech DX2 stopped-flow UV-visible spectrophotometer. All reported concentrations are those after mixing. Reaction of oxidized GB1-hCLK-1 (4 μM) and NADH (60 μM) in the presence of DMQ_2 (60 μM) was followed at 370 nm. Drive syringes and flow lines of the stopped-flow instrument were made anaerobic by flushing with at least 10 mL of an anaerobic solution of 4 mM sodium dithionite in 100 mM Tris, 10% glycerol, pH 7 buffer. Excess dithionite was removed by purging the syringes and flow lines with anaerobic buffer. Prior to conducting the stopped-flow experiments, a solution of 8 μM of GB1-hCLK-1 was incubated anaerobically with 120 μM of DMQ_2 for 30 min. The solution was transferred to a drive syringe and loaded into the anaerobic stopped flow instrument. This solution was mixed with an equal volume of 120 μM of NADH in 100 mM Tris, 10% glycerol, pH 7 buffer. The temperature was

maintained at 25 °C with a circulating water bath. The temperature of the reaction cell was verified by means of a thermocouple. Data were collected using a photomultiplier tube (PMT) with a tungsten lamp. Extinction coefficients at 370 nm for all reactants are as follows: oxidized GB1-hCLK-1, 4000 $M^{-1}cm^{-1}$; reduced GB1-hCLK-1, 1800 $M^{-1}cm^{-1}$; NADH, 2800 $M^{-1}cm^{-1}$; oxidized DMQ_2, 1900 $M^{-1}cm^{-1}$; and reduced DMQ_2, 1500 $M^{-1}cm^{-1}$. These values were used to fit time-dependent absorbance changes at 370 nm to one of two models shown in Scheme 1.[20]

Preparation of apo-GB1-hCLK-1

The expression and purification procedures were altered to obtain apo-GB1-hCLK-1. The $(NH_4)_2Fe(SO_4)\cdot 6H_2O$ was omitted during expression and 100 μM $(NH_4)_2Fe(SO_4)\cdot 6H_2O$ was replaced by 1 mM DTT in buffers A and B during the purification. No iron was detected in purified GB1-hCLK-1 with this procedure.

Mössbauer Spectroscopy

A 95.5% ^{57}Fe-enriched sample of GB1-hCLK-1 was prepared as reported previously.[14] The iron content for ^{57}Fe-enriched GB1-hCLK-1 was 2.0 ± 0.3. Oxidized GB1-hCLK-1 containing DMQ_0 was prepared by mixing the protein with 1.6 equivalents of the quinone and freezing the solution in a Mössbauer cup. Zero-field Mössbauer spectra were recorded at 78 K by using a conventional constant acceleration spectrometer equipped with a temperature controller maintaining temperatures within ± 0.1 K and a ^{57}Co radiation source in a Rh matrix. Isomer shifts are referred to α-Fe metal at room temperature. Data were collected for 48 h at 78 K using protein samples containing approximately 40 μg of ^{57}Fe. Data were fitted with a sum of Lorentzian quadrupole doublets by using a least-squares routine with WMOSS.

EPR Measurements

In order to confirm the absence of adventitious iron in the as-isolated GB1-hCLK-1 and to characterize Fe^{II}-Fe^{III} mixed-valent or semiquinone species, EPR spectroscopy was employed. A 1 mM solution of GB1-hCLK-1 (or GB1-hCLK-1/DMQ_n, n = 0 or 2) in 20 mM Tris, 10 % glycerol, pH 7.0 buffer was mixed with 250 or 500 μM of sodium dithionite (or NADH) under anaerobic conditions. Reaction of 500 μM oxidized GB1-hCLK-1 and 500 μM NADH in the presence of 500 μM DMQ_2 was rapidly freeze-quenched after mixing for 0.5, 1.5, and 5 s by spraying into a cold isopentane bath at -140 °C in order to characterize the transient formation of semiquinone or Fe^{II}-Fe^{III} mixed-valent species. X-band EPR spectra were recorded on a Bruker ESP 300 spectrometer equipped with an Oxford EPR 900 liquid helium cryostat. Data were recorded under the following conditions: temperature, 4.2 or 77 K; microwave frequency, 9.38-9.40 GHz; microwave power, 2 mW; modulation frequency, 100 kHz; and modulation amplitude, 5 G. EPR quantitation was performed by double integration under a non-saturating condition by using 325, 160, and 80 μM of Fe^{III}(EDTA) as a standard.

Results and Discussion

Expression of Human CLK-1 as a GB1 Fusion Protein

Spectroscopic and enzymatic studies of the membrane-bound protein human CLK-1 have been hampered by its limited solubility. To remedy this situation, we used the immunoglobulin binding domain of protein G (GB1) to create an N-terminal fusion of human CLK-1 (GB1-hCLK-1). The fusion protein improved both the expression level and the solubility of the enzyme.[15] A pET30a(+)-GBFusion vector containing the human *clk-1* gene was constructed having a small (6,367 Da) acidic (pI = 4.5) GB1 tag that is unlikely to interact with hCLK-1 (pI = 5.7) or alter its structure or ability to assembly the diiron center.

Another benefit of having the GB1 fusion at the N-terminus is that the hydrophilic GB1 moiety is synthesized prior to the target gene, which often aids in proper folding of the protein of interest. GB1-hCLK-1 was expressed and purified in *E. coli* in high yield, ~13 mg per liter of soluble fusion protein. SDS-PAGE analysis of purified GB1-hCLK-1 exhibited a single band corresponding to a protein mass ~26 kDa, which is consistent with the calculated molecular weight of 26,507 Da, as well as the value of 26,505 Da determined by MALDI-TOF (Supplementary Fig. S2). The solubility of the hCLK-1 membrane-bound enzyme was significantly improved, to 3 mM (in 20 mM Tris, 10% glycerol, pH 7.0), through construction of the N-terminal GB1 fusion protein. Based on size exclusion chromatography, GB1-hCLK-1 is dimeric in solution.

Characterization of the Diiron Center

Compared to that of apo-GB1-hCLK-1, the UV-vis spectrum of the expressed GB1-hCLK-1 protein displays an absorption band at 340 nm with $\varepsilon \sim 5300$ $M^{-1}cm^{-1}$ (Fig. 1). This optical feature is similar to that observed in mouse CLK-1 containing an N-terminal maltose-binding protein (MBP-mCLK-1),[14] which is typical of an oxo-bridged diiron(III) center.[21] Following addition of NaN_3, additional absorption bands at 342 and 450 nm appear (Fig. 1). The emergence of these optical features is consistent with other azide-adducts of carboxylate-bridged (μ-oxo)diiron(III) proteins, including stearoyl-acyl carrier protein Δ^9 desaturase (Δ9D) and hemerythrin.[22-23] The stoichiometry of Fe-to-GB1-hCLK-1 was determined to be 2.0(± 0.2):1, consistent with the present of a single diiron center. In order to further characterize this unit, we obtained the Mössbauer spectrum of a frozen solution of the protein that was 95.5% ^{57}Fe-enriched at 78 K and zero magnetic field. As shown in Fig. 2a, there are two signals with isomer shifts typical of carboxylate-bridged high-spin diiron(III) units (Table 1).[24-26] The simulation revealed two doublets best described as having isomer shifts (δ) of 0.47 ± 0.02 mm/s, with a corresponding quadrupole doublet (ΔE_Q) of 0.72 ± 0.02 mm/s (73%), and δ of 0.50 ± 0.02 mm/s, with $\Delta E_Q = 1.33 \pm 0.02$ mm/s (27%). Extensive studies of diiron model complexes suggest an assignment of these features to μ-hydroxo- and μ-oxo-diiron(III) centers, respectively.[21,27] Together, these distinctive UV-vis and Mössbauer characteristics provide strong evidence that the isolated CLK-1 enzyme contains a non-heme, carboxylate-bridged diiron(III) center in a mixture of oxo- and hydroxo-bridged forms, similar to that observed in MBP-mCLK-1.[14]

Analysis of the Mössbauer signal of the GB1-tagged hCLK-1 differs from that of MBP-mCLK-1 in a number of ways.[14] The ΔE_Q values of 0.72 (73%) and 1.33 (27%) mm/s for GB1-hCLK-1, and of 0.62 (59%) and 1.59 (41%) mm/s for MBP-mCLK-1, suggest that the protonation states of the solvent-derived oxygen ligands may differ slightly for these two protein constructs. The differences may be a result of the protein source, mouse vs. human, but may also arise from perturbations introduced by the relative large MBP tag (42 kDa, pI = 5.7). In addition, there was adventitious iron in the samples of MBP-mCLK-1, which had to be accounted for in the Mössbauer spectral fits. In contrast, there is no adventitious iron in GB1-hCLK-1, a conclusion that is supported by Mössbauer spectroscopy and the lack of a characteristic g = 4.3 signal in the EPR spectrum of oxidized GB1-hCLK-1 (Supplementary Fig. S3). Moreover, the absence of adventitious Fe demonstrates the value of GB1 as a solubility-enhancement tag for the enzymatic study.

Hydroxylation of DMQ derivatives

CLK-1 has been proposed as a DMQ hydroxylase because of the accumulation of DMQ_9 in Δ*clk-1* mutants of *C. elegans* and mice.[7] We therefore prepared 2-methoxy-5-methyl-1,4-benzoquinone (DMQ_0) to evaluate its potential to serve as a substrate for hydroxylation by CLK-1 (Chart 1). The product formed in the reaction of 5 μM GB1-hCLK-1, 1 mM DMQ_0, and 1 mM NADH, characterized by GC-MS, indicated that GB1-hCLK-1 catalyzes the

hydroxylation of DMQ_0 to generate DMQ_0-OH (Fig. 3). Based on the time course of DMQ_0-OH formation using GB1-hCLK-1, an apparent k_{cat} of 2.3 min^{-1} was calculated (Supplementary Fig. S4).

The steady state activity of GB1-hCLK-1 was investigated by an NADH consumption assay. In contrast to the negligible consumption of NADH in the reaction of 5 µM GB1-hCLK-1 with 200 µM NADH (0.2 ± 0.1 µM/min), the NADH consumption rate was 12.7 ± 0.6 µM/min in the presence of 1 mM DMQ_0 (Table 2). This enhanced NADH consumption suggests that continuous and catalytic reduction of the diiron center by NADH upon addition of DMQ_0 occurs to activate dioxygen for DMQ_0 hydroxylation. There was no DMQ_0 hydroxylation or NADH consumption when apo-GB1-hCLK-1 was examined, further corroborating the requirement for a carboxylate-bridged diiron center to activate O_2 and oxidize DMQ_0.

As shown in Fig. 4, a steady state activity analysis of NADH consumption using GB1-hCLK-1 in the presence of DMQ_0 displayed typical Michaelis-Menten kinetics, with $K_M = 68.1$ µM, $V_{max} = 12.8$ µM/min, and $k_{cat}/K_M = 37.6$ min^{-1}mM^{-1}. The absence of a kinetic solvent isotope effect (KSIE) for k_{cat} measured in H_2O vs. D_2O ($k_H/k_D = 1.0$) suggests that protonation/deprotonation is not involved in the rate-determining step during the catalytic cycle. Rather, an intermolecular isotope effect of 3 on K_M ($^DK = {}^DK_M/{}^HK_M$), was determined.[28]

The binding of DMQ_0 to GB1-hCLK-1 was characterized by Mössbauer spectroscopy, and similar isomer shift values were observed in the absence and presence of the substrate (Fig. 2b and Table 1). The two quadrupole splitting parameters changed from 0.72 and 1.33 mm/s to 0.61 and 1.24 mm/s upon addition of DMQ_0 to GB1-hCLK-1. Unlike the significant perturbation of the diiron active site by NaN_3 revealed by optical spectroscopy (Fig. 1), similar absorption spectra were obtained for oxidized GB1-hCLK-1 in the absence and presence of DMQ_0 or DMQ_0-OH. A comparison of substrate- and product-exposed GB1-hCLK-1 spectra with that of the NaN_3 GB1-hCLK-1 adduct indicates comparatively minor perturbation of the diiron(III) active site (Supplementary Fig. S5). Unlike the formation of a broad optical absorption band centered at 580 nm observed for product (catecholate)-bound ToMOH,[29] the minor perturbation of the optical spectrum excludes DMQ_0 (or DMQ_0-OH) coordination to the active site iron atoms. These results support the previous proposal that substrate binds to the Glu_{22}/His_{110}/Tyr_{111} triplet of amino acids of CLK-1 rather than directly to the diiron site (Supplementary Fig. S1).[10]
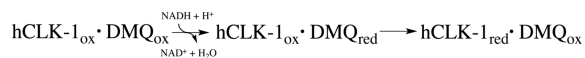
In order to assess the influence of an isoprenoid side chain on substrate binding and steady state activity, DMQ_2 was prepared and evaluated as a substrate (Chart 1). The K_M of 33.8 µM for DMQ_2, by comparison to the value of 68.1 µM for DMQ_0, reveals that inclusion of an isoprenoid side chain increases the binding affinity of a quinone substrate to GB1-CLK-1 (Fig. 4). Moreover, the increase in V_{max} from 12.8 µM/min to 39.2 µM/min and k_{cat}/K_M from 37.6 min^{-1}mM^{-1} to 232.0 min^{-1}mM^{-1} upon replacing DMQ_0 with DMQ_2 demonstrates that the isoprenoid side chain not only enhances enzymatic hydroxylation activity but also improves catalytic efficiency (Table 2). A similar dependence of catalytic efficiency on the length of acyl-chain of substrate is observed in Δ^9 desaturase.[30] Although a significant enhancement in GB1-hCLK-1 catalytic efficiency was expected using the natural substrate, DMQ_{10}, the decrease in solubility of DMQ substrates when the isoprenoid side chain was increased from DMQ_0 (~3 mM) to DMQ_2 (~500 µM) prohibited the use of DMQ_n substrates with longer isoprenoid side chains. The association of DMQ_{10} and CLK-1 with the mitochondrial membrane through hydrophobic interactions most likely provides an orientational preference for facile electron transfer and DMQ-hydroxylation.

Substrate-Mediated Electron Transfer

Because there is negligible NADH consumption by GB1-hCLK-1 in the absence of quinone, there appears to be substrate-gated electron transfer from NADH to the diiron center, leading to subsequent O_2 activation and DMQ hydroxylation. Reductive titrations of GB1-hCLK-1 by sodium dithionite or NADH were therefore performed under anaerobic conditions in order to obtain more direct evidence for substrate-gated electron transfer. Titrations of GB1-hCLK-1 with sodium dithionite revealed that two electrons are required for complete reduction of the diiron center, as monitored by a decrease in the intensity of the putative oxo-to-Fe^{III} charge transfer band at 340 nm (Fig. 5). This optical change further supports the conclusion that each GB1-hCLK-1 contains a single carboxylate-bridged diiron center. Addition of O_2-saturated buffer to reduced GB1-hCLK-1 resulted in nearly quantitative reoxidation of diiron center (93% recovery, Supplementary Fig. S6). In contrast to the inability to reduce the diiron center in GB1-hCLK-1 by NADH in the absence of substrate, reduction of diiron center by NADH occurs in the presence of one equivalent of DMQ_0 as indicated by the decrease of A_{340}. These results support substrate-gated electron transfer (Fig. 5). The absence of a characteristic EPR signal for an Fe^{II}-Fe^{III} mixed-valent or semiquinone during the reductive titration of oxidized GB1-hCLK-1 with dithionite or DMQ_0/NADH excludes the formation of Fe^{II}-Fe^{III} mixed-valent or semiquinone species in GB1-hCLK-1. The attempt to characterize the transient formation of such species is discussed below.

In Δ9D, a substrate-induced conformational change at the diiron center induced a positive shift in the reduction potential from –320 mV to –210 mV to facilitate its reduction by NADH (reduction potential -320 mV, vs NHE).[31] In order to investigate whether DMQ_0-binding similarly promotes NADH reduction of the diiron center in GB1-hCLK-1, the redox potential of the diiron center was determined by reductive titration using indicator dyes (Fig. 6). Unlike the thermodynamic gating of catalysis in Δ9D, the reduction potential of the diiron center in GB1-hCLK-1, 3 mV vs NHE, is sufficiently high such that NADH reduction is thermodynamically facile in the absence of substrate. This result suggests that a kinetic barrier prevents reduction of the diiron center and that binding of DMQ_0 to GB1-hCLK-1 in some manner provides a pathway for electron transfer by NADH.

We considered two possible mechanisms for this process, (i) quinone-mediated reduction by NADH (Schemes 1b and 1c) and (ii) quinone-gated conformational change of GB1-hCLK-1 for reduction by NADH (Scheme 1b'). In an attempt to distinguish between these two pathways, the reduction of oxidized GB1-hCLK-1 in the presence of DMQ_2 by NADH under pre-steady-state conditions was investigated. Using this method, we observed that the decay in A_{370} did not fit well to a single exponential. Instead, the data fit well to a sum of two exponentials describing the substrate-mediated reduction process (). Fitting the data in this manner return rate constants $k_1' = 1.15 \pm 0.04$ s^{-1} and $k_2 = 0.046 \pm 0.002$ s^{-1} (Figure S7).

$$\text{hCLK-1}_{ox}\cdot \text{DMQ}_{ox} \underset{NAD^+ + H_2O}{\overset{NADH + H^+}{\rightleftharpoons}} \text{hCLK-1}_{ox}\cdot \text{DMQ}_{red} \longrightarrow \text{hCLK-1}_{red}\cdot \text{DMQ}_{ox}$$

(2)

In order to characterize the transient formation of semiquinone or Fe^{II}-Fe^{III} mixed-valent species in the reduction of oxidized GB1-hCLK-1 by NADH, the reaction of oxidized GB1-hCLK-1 with NADH in the presence of DMQ_2 was also rapid-freeze quenched after mixing for 0.5, 1.5, and 5 s. The absence of an EPR signal characteristic of a semiquinone or Fe^{II}-Fe^{III} species supports quinone-mediated two-electron reduction of the diiron(III) center in GB1-hCLK-1 by NADH (Scheme 1b and 1c). Utilization of the intrinsic redox capability of

a hydroquinone to mediate such two-electron transfer processes has been previously reported.[6,32-33] Intermolecular electron transfer from Complex I or II to Complex III in the inner mitochondrial membrane of eukaryotes is similarly promoted, and hydroquinone-mediated intramolecular electron transfer occurs in the bacterial reaction center from *Rb. Sphaeroides*.[6,32-33] The primary quinone, Q_A, is reduced by the excited bacterichlorophyll dimer (D) and then the reduced Q_A^- further transfers an electron to the secondary quinone, Q_B ($DQ_AQ_B \rightarrow D^+Q_A^-Q_B \rightarrow D^+Q_AQ_B^-$).

NADH does not react with either hCLK-1_{ox} or its quinone substrates in the absence of the enzyme. In the presence of hCLK-1_{ox} and DMQ_{ox}, however, the enzyme becomes reduced, implying the transient formation of DMQ_{red} and quinone-mediated electron transfer. We presume that this activity involves solvent-exchangeable hydrogen bonding interactions between the $Glu_{22}/His_{110}/Tyr_{111}$ amino acid triad in GB1-hCLK-1 and quinones, which promotes their reduction by NADH. The enhanced reduction of quinones by NADH derivatives through hydrogen bonding interactions has precedence in the literature.[34]

Conclusion

We report the high-yield expression and purification of soluble human CLK-1 in *E. coli* as an N-terminal GB1 fusion. UV-vis and Mössbauer spectroscopic studies of this protein provide unambiguous evidence that human CLK-1 belongs to the carboxylate-bridged diiron protein family of proteins and activates O_2 for DMQ hydroxylation at the diiron center. Human CLK-1 is the first membrane-bound diiron protein in humans that functions as a hydroxylase.

The binding of DMQ_n substrates in GB1-hCLK-1 gates and mediates reduction of the diiron center by NADH without an additional reductase protein component. Substrate-gated reduction of a diiron center for O_2 activation and DMQ hydroxylation in human CLK-1 conveys specificity and prevents undesired consumption of NADH in mitochondria. The development of a highly efficient *E. coli* expression system to generate sufficient quantities of soluble human CLK-1 with GB1 fusion protein for further study should help to unravel the role of CLK-1, as well as its roles in the biosynthesis of ubiquinone and the aging process.

Supplementary Material

Refer to Web version on PubMed Central for supplementary material.

Acknowledgments

Abbreviations

GB1	immunoglobulin binding domain of protein G
DMQ	5-demethoxyubiquinone
UQ	ubiquinone
sMMO	soluble methane monooxygenase

ToMO	toluene monooxygenase
PH	phenol hydroxylase
DMQ$_0$	2-Methoxy-5-methyl-1,4-benzoquinone
DMQ$_0$-OH	2-methoxy-3-hydroxyl-5-methyl-1,4-benzoquinone
PCR	polymerization chain reaction
IPTG	isopropyl β-D-1-thiogalactopyranoside
PMSF	phenylmethanesulfonylfluoride
SDS	sodium dodecyl sulfate
PAGE	polyacrylamide gel electrophoresis
BSA	bovine serum albumin
NADH	nicotinamide adenine dinucleotide

References

1. Kirkwood TB. A systematic look at an old problem. Nature. 2008; 451:644–647. [PubMed: 18256658]

2. Lakowski B, Hekimi S. Determination of life-span in *Caenorhabditis elegans* by four clock genes. Science. 1996; 272:1010–1013. [PubMed: 8638122]

3. Ewbank JJ, Barnes TM, Lakowski B, Lussier M, Bussey H, Hekimi S. Structural and functional conservation of the *Caenorhabditis elegans* timing gene *clk-1*. Science. 1997; 275:980–983. [PubMed: 9020081]

4. Lapointe J, Hekimi S. Early mitochondrial dysfunction in long-lived *Mclk1*$^{+/-}$ mice. J. Biol. Chem. 2008; 283:26217–26227. [PubMed: 18635541]

5. Levavasseur F, Miyadera H, Sirois J, Tremblay ML, Kita K, Shoubridge E, Hekimi S. Ubiquinone is necessary for mouse embryonic development but is not essential for mitochondrial respiration. J. Biol. Chem. 2001; 276:46160–46164. [PubMed: 11585841]

6. Ernster L, Forsmark-Andree P. Ubiquinol: an endogenous antioxidant in aerobic organisms. Clin. Investig. 1993; 71:S60–65.

7. Miyadera H, Amino H, Hiraishi A, Taka H, Murayama K, Miyoshi H, Sakamoto K, Ishii N, Hekimi S, Kita K. Altered quinone biosynthesis in the long-lived *clk-1* mutants of *Caenorhabditis elegans*. J. Biol. Chem. 2001; 276:7713–7716. [PubMed: 11244089]

8. Tran UC, Clarke CF. Endogenous synthesis of coenzyme Q in eukaryotes. Mitochondrion. 2007; 7(Suppl):S62–71. [PubMed: 17482885]

9. Stenmark P, Grunler J, Mattsson J, Sindelar PJ, Nordlund P, Berthold DA. A new member of the family of di-iron carboxylate proteins. Coq7 (clk-1), a membrane-bound hydroxylase involved in ubiquinone biosynthesis. J. Biol. Chem. 2001; 276:33297–33300. [PubMed: 11435415]

10. Rea S. CLK-1/Coq7p is a DMQ mono-oxygenase and a new member of the di-iron carboxylate protein family. FEBS Lett. 2001; 509:389–394. [PubMed: 11749961]

11. Nordlund P, Eklund H. Structure and function of the Escherichia coli ribonucleotide reductase protein R2. J Mol Biol. 1993; 232:123–164. [PubMed: 8331655]

12. Kurtz DM. Structural similarity and functional diversity in diiron-oxo proteins. J. Biol. Inorg. Chem. 1997; 2:159–167.

13. Arnold K, Bordoli L, Kopp J, Schwede T. The SWISS-MODEL workspace: a web-based environment for protein structure homology modelling. Bioinformatics. 2006; 22:195–201. [PubMed: 16301204]

14. Behan RK, Lippard SJ. The aging-associated enzyme CLK-1 is a member of the carboxylate-bridged diiron family of proteins. Biochemistry. 2010; 49:9679–9681. [PubMed: 20923139]

15. Zhou P, Wagner G. Overcoming the solubility limit with solubility-enhancement tags: successful applications in biomolecular NMR studies. J. Biomol. NMR. 2010; 46:23–31. [PubMed: 19731047]

16. Bernini R, Mincione E, Barontini M, Provenzano G, Setti L. Obtaining 4-vinylphenols by decarboxylation of natural 4-hydroxycinnamic acids under microwave irradiation. Tetrahedron. 2007; 63:9663–9667.

17. van der Klei A, de Jong RLP, Lugtenburg J, Tielens AGM. Synthesis and spectroscopic characterization of [1'-C-14]ubiquinone-2, [1'-C-14]-5-demethoxy-5-hydroxyubiquinone-2, and [1'-C-14]-5-demethoxyubiquinone-2. Eur. J. Org. Chem. 2002:3015–3023.

18. Blazyk JL, Lippard SJ. Expression and characterization of ferredoxin and flavin adenine dinucleotide binding domains of the reductase component of soluble methane monooxygenase from *Methylococcus capsulatus* (Bath). Biochemistry. 2002; 41:15780–15794. [PubMed: 12501207]

19. Kopp DA, Gassner GT, Blazyk JL, Lippard SJ. Electron-transfer reactions of the reductase component of soluble methane monooxygenase from Methylococcus capsulatus (Bath). Biochemistry. 2001; 40:14932–14941. [PubMed: 11732913]

20. Beauvais LG, Lippard SJ. Reactions of the peroxo intermediate of soluble methane monooxygenase hydroxylase with ethers. J. Am. Chem. Soc. 2005; 127:7370–7378. [PubMed: 15898785]

21. Kurtz DM. Oxo- and hydroxo-bridged diiron complexes: a chemical perspective on a biological unit. Chem. Rev. 1990; 90:585–606.

22. Fox BG, Shanklin J, Somerville C, Munck E. Stearoyl-acyl carrier protein Δ^9 desaturase from Ricinus communis is a diiron-oxo protein. Proc. Natl. Acad. Sci. 1993; 90:2486–2490. [PubMed: 8460163]

23. Richard C, Reem EIS. Spectroscopic studies of the binuclear ferrous active site of deoxyhemerythrin: coordination number and probable bridging ligands for the native and ligand-bound forms. J. Am. Chem. Soc. 1987; 109:1216–1226.

24. Vu VV, Emerson JP, Martinho M, Kim YS, Munck E, Park MH, Que L Jr. Human deoxyhypusine hydroxylase, an enzyme involved in regulating cell growth, activates O_2 with a nonheme diiron center. Proc. Natl. Acad. Sci. 2009; 106:14814–14819. [PubMed: 19706422]

25. Xing G, Hoffart LM, Diao Y, Prabhu KS, Arner RJ, Reddy CC, Krebs C, Bollinger JM Jr. A coupled dinuclear iron cluster that is perturbed by substrate binding in myo-inositol oxygenase. Biochemistry. 2006; 45:5393–5401. [PubMed: 16634620]

26. Wallar BJ, Lipscomb JD. Dioxygen Activation by Enzymes Containing Binuclear Non-Heme Iron Clusters. Chem. Rev. 1996; 96:2625–2658. [PubMed: 11848839]

27. Armstrong WH, Lippard SJ. Reversible Protonation of the Oxo Bridge in a Hemerythrin Model-Compound-Synthesis, Structure, and Properties of (μ-Hydroxo)mis(μ-acetato)bis[hydrotris(1-pyrazolyl)borato]diiron(III), [(HB(pz)$_3$)Fe(OH)(O$_2$CCH$_3$)$_2$Fe(HB(pz)$_3$)]$^+$. J. Am. Chem. Soc. 1984; 106:4632–4633.

28. Bell LC, Guengerich FP. Oxidation kinetics of ethanol by human cytochrome P450 2E1. J. Biol. Chem. 1997; 272:29643–29651. [PubMed: 9368031]

29. Murray LJ, Naik SG, Ortillo DO, Garcia-Serres R, Lee JK, Huynh BH, Lippard SJ. Characterization of the arene-oxidizing intermediate in ToMOH as a diiron(III) species. J. Am. Chem. Soc. 2007; 129:14500–14510. [PubMed: 17967027]

30. Haas JA, Fox BG. Role of hydrophobic partitioning in substrate selectivity and turnover of the Ricinus communis stearoyl acyl carrier protein Δ^9 desaturase. Biochemistry. 1999; 38:12833–12840. [PubMed: 10504253]

31. Reipa V, Shanklin J, Vilker V. Substrate binding and the presence of ferredoxin affect the redox properties of the soluble plant Δ^9-18:0-acyl carrier protein desaturase. Chem. Comm. 2004:2406–2407. [PubMed: 15514788]

32. Graige MS, Feher G, Okamura MY. Conformational gating of the electron transfer reaction Q$_A^-$Q$_B$ -> Q$_A$Q$_B^-$ in bacterial reaction centers of *Rhodobacter sphaeroides* determined by a driving force assay. Proc. Natl. Acad. Sci. 1998; 95:11679–11684. [PubMed: 9751725]

33. Graige MS, Paddock ML, Bruce JM, Feher G, Okamura MY. Mechanism of Proton-Coupled Electron Transfer for Quinone (Q$_B$) Reduction in Reaction Centers of *Rb. Sphaeroides*. J. Am. Chem. Soc. 1996; 118:9005–9016.

34. Yuasa J, Yamada S, Fukuzumi S. One-step versus stepwise mechanism in protonated amino acid-promoted electron-transfer reduction of a quinone by electron donors and two-electron reduction by a dihydronicotinamide adenine dinucleotide analogue. Interplay between electron transfer and hydrogen bonding. J. Am. Chem. Soc. 2008; 130:5808–5820. [PubMed: 18386924]
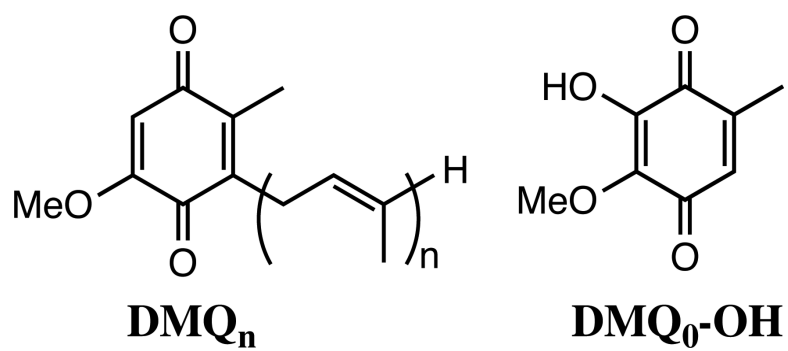
Chart 1.
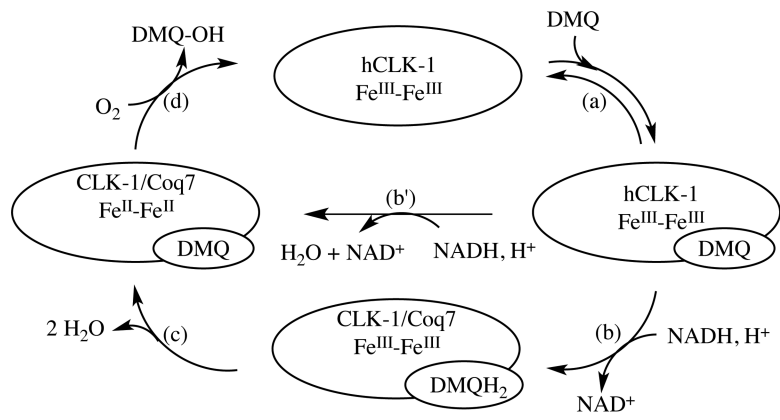
Scheme 1.
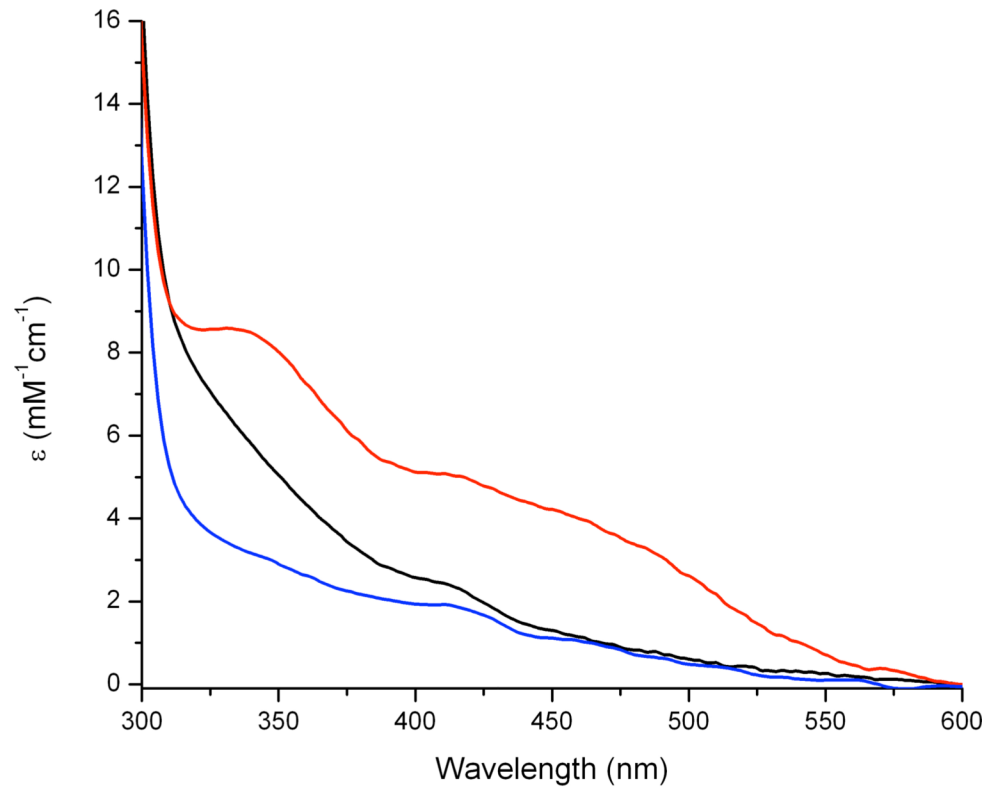
Figure 1.
UV-vis spectra of expressed GB1-hCLK-1 (black), after addition of NaN_3 (red), and apo-GB1-hCLK-1 (blue).

(a)
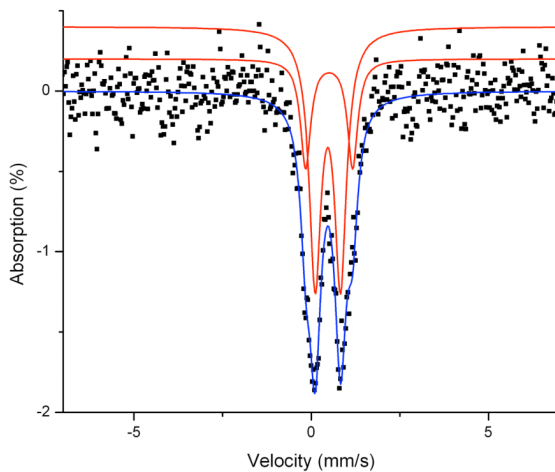
(b)
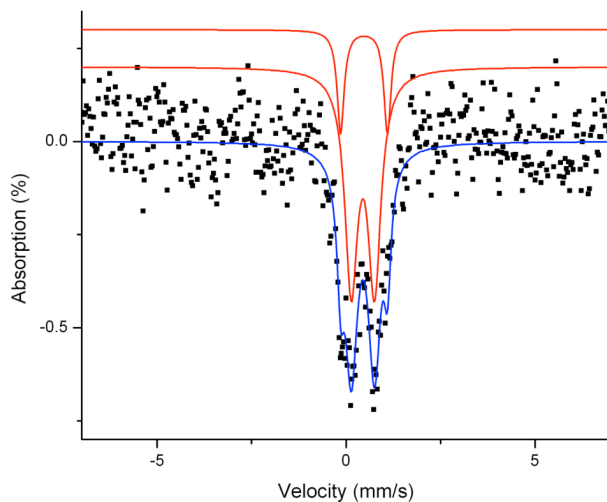
Figure 2.
DMQ_0 binding perturbs the oxidized diiron center in GB1-hCLK-1 as revealed by Mössbauer spectroscopy. (a) Mössbauer spectrum of 1 mM oxidized GB1-hCLK-1 without DMQ_0. (b) Mössbauer spectrum of 1 mM oxidized GB1-hCLK-1 in the presence of 1.6 mM DMQ_0. The red lines are simulated spectra of the components, which combine as indicated by the blue line overlaid on the experimental spectrum.

(a)
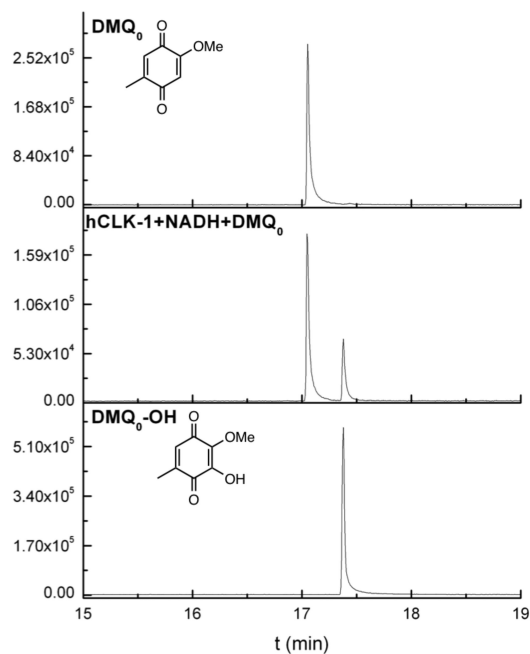
(b)
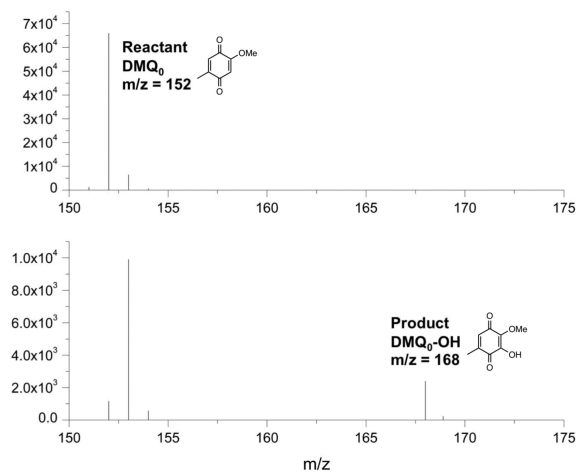
Figure 3.
GB1-hCLK-1 catalyzes the hydroxylation of DMQ_0. The product generated in the reaction of 5 µM GB1-hCLK-1, 1 mM DMQ_0 and 1 mM NADH is identified by GC-MS. (a) GC-MS chromatograph of DMQ_0 (top), reaction product (middle), and DMQ_0-OH (bottom). (b) MS spectra of DMQ_0 (top) and reaction product, DMQ_0-OH (bottom).
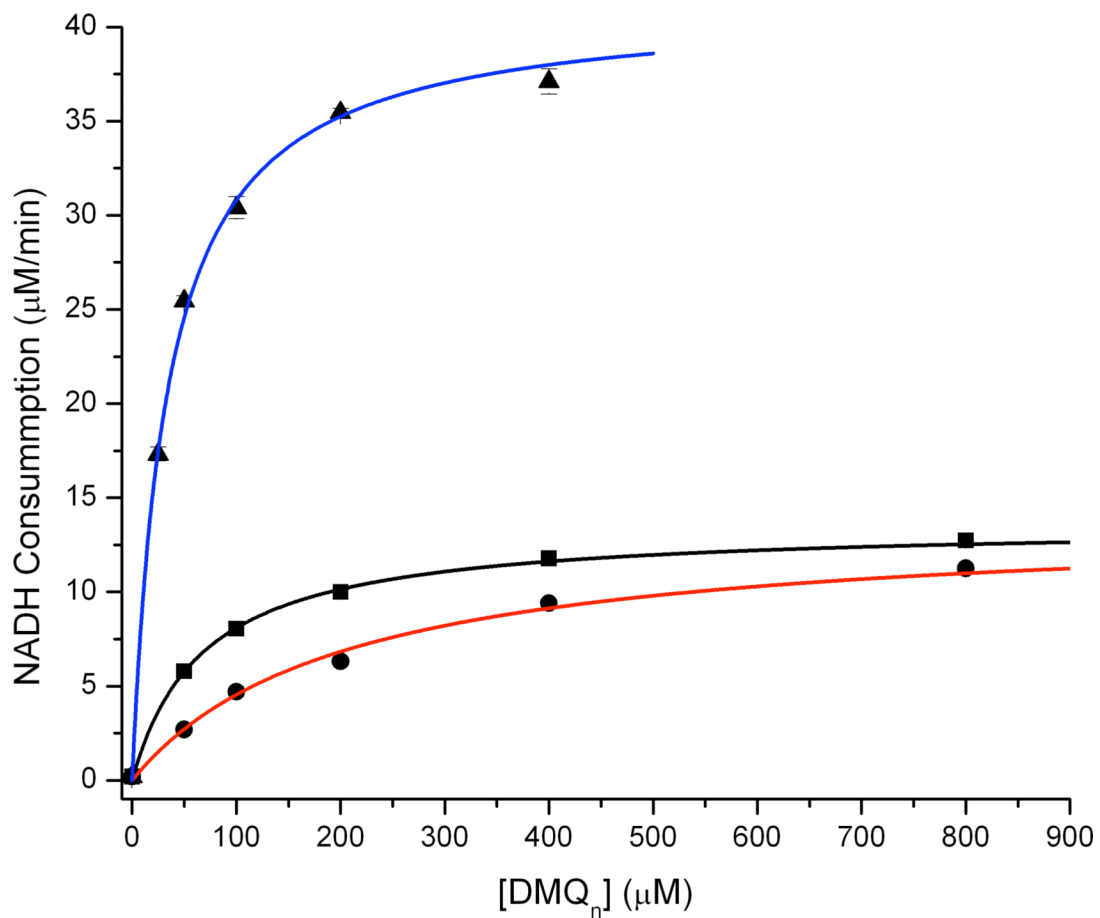
Figure 4.
Steady state activity of GB1-hCLK-1 based on an NADH consumption assay. DMQ_n was used as substrate (n = 0, black and red; or n = 2, blue). To check for a possible kinetic solvent isotopic effect, NADH consumption in the presence of GB1-hCLK-1 and DMQ_0 was carried out in H_2O (black) and D_2O (red). The NADH consumption rate was fit with Michaelis-Menten kinetics, as indicated by the solid lines.
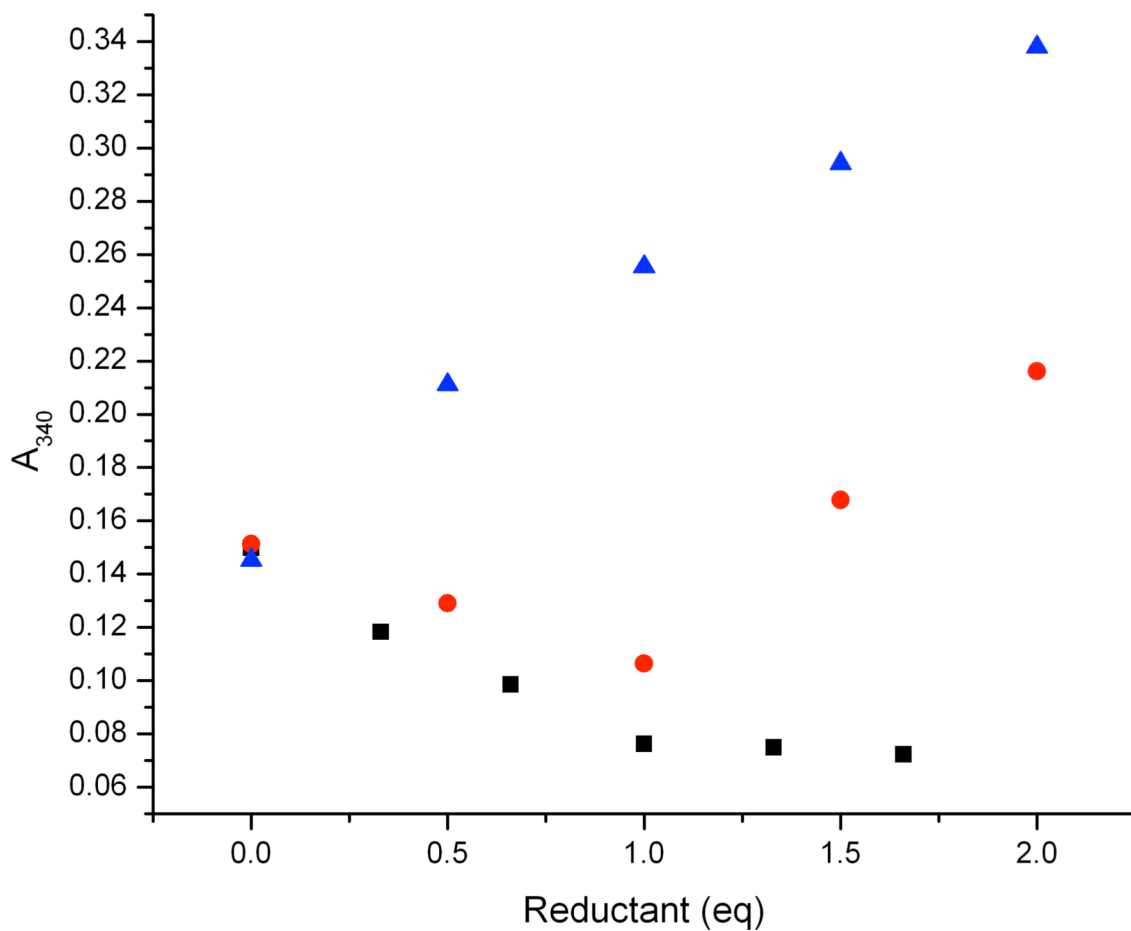
Figure 5.
Substrate-gated reduction of the diiron center in GB1-hCLK-1. The reduction of the diiron(III) center in resting state GB1-hCLK-1 was monitored by the decay of the optical band at 340 nm. Compared to the reduction of diiron center by dithionite (black) and the lack of NADH reactivity with GB1-hCLK-1 (blue), reduction of the diiron center by NADH in the presence of DMQ_0 demonstrates substrate-gated electron transfer from NADH to diiron center in GB1-hCLK-1 (red).
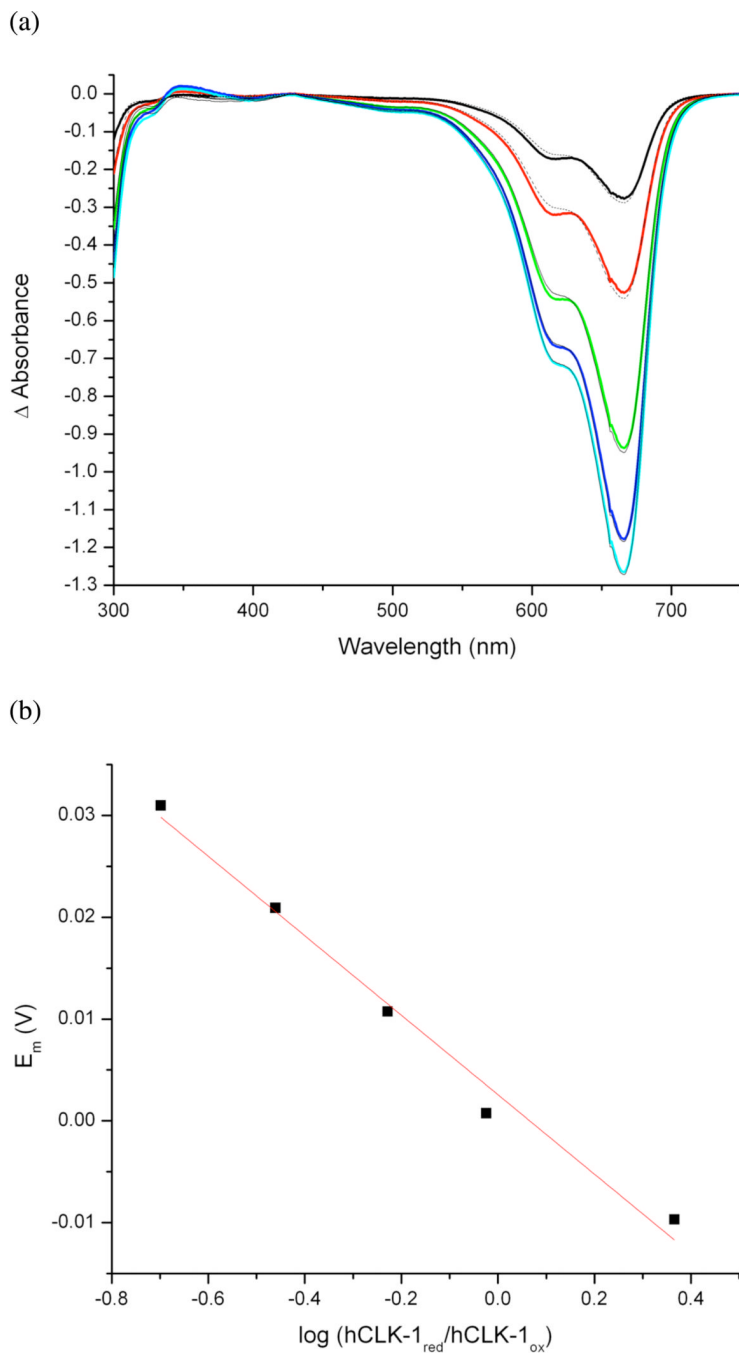
(a)

(b)

Figure 6.
Determination of the redox potential of the diiron center in GB1-hCLK-1. (a)Difference spectra for a reductive titration of 20 μM GB1-hCLK-1 and 20 μM methylene blue by 500 μM dithionite at pH 7.0 and 25 °C. Spectra correspond to the addition of 5, 10, 15, 20, and 25 μL of ca. 500 μM dithionite, respectively. Fits are shown as dashed lines. (b) Plot of the potential derived from log (dye$_{red}$/dye$_{ox}$) vs log (CLK-1$_{red}$/CLK-1$_{ox}$). The solid line indicates a fit to the modified Nernst equation (eq 1, see text).[18-19] The *y*-intercept of 3 mV (vs NHE) represents the redox potential of GB1-hCLK-1.

Table 1

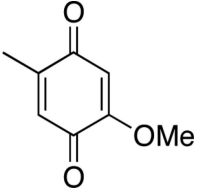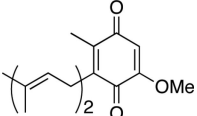Mössbauer Parameter for Carboxylate-Bridged Diiron Enzymes from Mammalians[a,b]

protein	isomer shift (δ) (mm/s)	quadruple splitting (ΔE_Q) (mm/s)	ref
Human	0.47	0.72	this work
CLK-1 no DMQ_0	0.50	1.33	
Human	0.45	0.61	this work
CLK-1 with DMQ_0	0.48	1.24	
Human	0.55	1.16	18b
DOHH	0.58	0.88	
Mouse	0.47	1.32	18c
MIOX	0.49	0.63	

[a] Abbreviation: DOHH, deoxyhypusine hydroxylase; MIOX, *myo*-inositol oxygenase.

[b] Standard deviation for isomer shift and quadruple splitting is 0.02 mm/s.

Table 2

NADH consumption rates, V_{max}, K_M and k_{cat}/K_M for GB1-hCLK-1 in the absence and presence of DMQ_0 or DMQ_2.

Substrate	NADH Consumption (μM/min)[a]	V_{max} (μM/min)	K_M (μM)	k_{cat}/K_M (mM^{-1}min^{-1})
none	0.2 ± 0.1	-	-	-
DMQ$_0$	12.7 ± 0.6	12.8^e 12.6^f	68.1^e 204.0^f	37.6^e 12.4^f
DMQ$_2$	37.1 ± 4.2^b 36.0 ± 4.8^c 34.9 ± 3.5^d	39.2	33.8	232.0

[a] 5 μM of GB1-hCLK-1, 200 μM of NADH, and 1mM of DMQ$_0$ or 400 μM of DMQ$_2$ were used.

[b] pre-mix GB1-hCLK-1 and DMQ$_2$ followed by addition of NADH.

[c] pre-mix GB1-hCLK-1 and NADH followed by addition of DMQ$_2$.

[d] pre-mix DMQ$_2$ and NADH followed by addition of GB1-hCLK-1.

[e] Reaction was performed in 20 mM Tris, pH 7.0.

[f] Reaction was performed in duteriated Tris buffer.